JOURNAL OF MATERIALS SCIENCE 26 (1991) 1803–1807

Sinter-forged $YBa_2Cu_3O_{7-x}$ superconducting ceramics from the spray-roasted powders

GUN YONG SUNG, C. B. CARTER
Department of Materials Science and Engineering, Bard Hall, Cornell University, Ithaca, NY 14853, USA

DOO HI CHO, CHONG HEE KIM
Department of Materials Science and Engineering, Korea Advanced Institute of Science and Technology, P.O. Box 131 Cheongryang, Seoul, Korea

The effect of applying a uniaxial stress, while varying the temperature and the time of sinter-forging, on the microstructure and critical current density of the sinter-forged $YBa_2Cu_3O_{7-x}$ ceramics has been investigated. Spray-roasted powders from a nitrate-based feed solution were prepared as the starting materials. By applying a relatively low uniaxial stress (2 MPa), the sintered density increased up to 95% of the maximum value. Critical current densities of between 360 and 420 A cm^{-2} were obtained for the sinter-forged samples which are significantly higher than values reported for pressureless-sintered samples prepared from solid-state reacted powders (typically 70 A cm^{-2}). This increase in the density of the material and the critical current density can be explained by the alignment of the elongated $YBa_2Cu_3O_{7-x}$ grains under applied uniaxial stress during sintering. The elongated $YBa_2Cu_3O_{7-x}$ grains have been characterized by transmission electron microscopy.

1. Introduction

The low critical current density is one of the main problems limiting with the application of polycrystalline $YBa_2Cu_3O_{7-x}$ superconductors. It is known that several factors contribute to the origins of the low critical current density. These factors can be summarized as follows.

1. The critical current density of $YBa_2Cu_3O_{7-x}$ single crystal is anisotropic (the value perpendicular to the c-axis is larger than that parallel to the c-axis) [1, 2].
2. The grain boundaries behave as weak-links which limit the maximum transport current between adjacent grains [3].
3. The sintered density is low (80%–85% theoretical maximum value, TD) [4].
4. Non-superconducting phases are often present (e.g. weakly superconducting grains, insulating layers at the grain boundaries, voids, and microcracks) [5].

Unfortunately, factor 1 is an intrinsic property of $YBa_2Cu_3O_{7-x}$ single crystal so that the anisotropic current-carrying capability cannot be avoided. But the difficulties due to the other three factors can be alleviated. Reducing the number of particularly deleterious grain boundaries by the alignment of the elongated $YBa_2Cu_3O_{7-x}$ grains normal to their c-axis can minimize the effect of the weak-link nature of the grain boundary on the polycrystalline ceramics.

The simultaneous application of pressure and temperature (sinter-forging) can enhance densification rates, reduce densification temperatures, and produce a textured microstructure [6, 7]. During the process, the plungers are slowly pressed together at the required temperature, allowing free movement of the specimen in the lateral direction. Thus, the c-planes (the planes perpendicular to the c-axis) of the elongated $YBa_2Cu_3O_{7-x}$ grains tend to align perpendicular to the forging direction. In addition to texturing, densification to near 95% TD can be obtained in the polycrystalline $YBa_2Cu_3O_{7-x}$ ceramics using this approach. The sinter-forging process has been applied previously to produce the textured barium ferrite ceramics [8, 9] where the densification and the creep mechanism of powder compacts [10–14] were studied. The technique is particularly attractive because it provides greater control of the dimension and shape of the article. Hot-pressing [15, 16], hot isostatic pressing [17], hot extrusion [18], shock compaction [19], and pressureless sintering by addition of Ag_2O [20] have also been reported as possible methods for developing the desired textured microstructure for the high-T_c superconducting ceramics. Recently, the critical current density of the bulk $YBa_2Cu_3O_{7-x}$ superconductors has been remarkably improved by melt process [21–24]. Although the highest critical current density for a bulk sample (up to 75 000 A cm^{-2}) was obtained by this process, the experimental difficulties, the reproducibility of the method and the limited size of the samples were significant drawbacks.

The aim of the present study is to advance the understanding of these sinter-forged $YBa_2Cu_3O_{7-x}$ superconductors. The effects of varying the applied

0022–2461/91 $03.00 + .12

uniaxial stress, the sinter-forging temperature and processing time on the densification and critical current density of the sinter-forged samples has been investigated. Spray-roasted powders from nitrate feed solutions were prepared as the starting materials. The crystallographic orientation relationship between the elongated $YBa_2Cu_3O_{7-x}$ grains and the stress axis has been characterized on the microscopic scale using selected-area diffraction (SAD) and high-resolution imaging in the TEM, and macroscopically using X-ray diffraction.

2. Experimental procedure

$Y(NO_3)6H_2O$, $Ba(NO_3)_2$, and $Cu(NO_3)_23H_2O$, were dissolved in distilled water and the solution sprayed on to the hot tray at 300 °C (the spray-roasting process). This spray-roasted powder was calcined at 800 °C for 5 h in a N_2 atmosphere and then ground and recalcined at 850 °C for 5 h in an O_2 atmosphere. For comparison, solid-state-reacted powder was also prepared by the mechanical mixing and calcining of the mixture of Y_2O_3, $BaCO_3$, and CuO.

The powder was compacted uniaxially under a pressure of 450 kg cm^{-2} and isostatically under a pressure of 1470 kg cm^{-2}. Sinter-forging was conducted in a vertical tube furnace with a kanthal heating element. The pellets were placed between alumina rams, but separated from the rams by a sintered MgO plate. Forging was carried out at 860, 880 and 900 °C under a constant stress of 0, 1 and 2 MPa in air. The sinter-forging time was varied between 0 and 20 h. The samples were then annealed at 600 °C for 5 h, followed by 450 °C for 10 h, in a flowing O_2 atmosphere with a flowing rate of 30 cm^3 min^{-1}.

The density of each sinter-forged sample was measured by Archimedes method using kerosene rather than of water. X-ray diffraction measurements were performed on the calcined powders from both preparation routes. The texture of each sinter-forged sample was evaluated by X-ray diffraction using CuK_α radiation using a cross-section cut perpendicular to the sinter-forging axis. The diffracted intensities from the (0 0 3), (0 0 5), and (0 0 6) planes were compared to the intensity from the (1 0 3) plane as a standard. Bar-shaped samples were cut from the sinter-forged pellets with the long axis perpendicular to the forging axis in order to measure the resistance versus temperature characteristics and the transport critical current density, J_c.

TEM samples were prepared by mechanical polishing and dimpling, followed by ion-milling (VCR Group Maxmill) with Ar^+ at 5 kV using a cold stage (77 K) until perforation. Images and SAD patterns were recorded using a Jeol 1200EX (120 kV) transmission electron microscope.

3. Results and discussion

X-ray diffraction patterns of the spray-roasted powder and the solid-state-reacted powder after calcination are shown in Fig. 1. The pattern from the spray-roasted powder shows only the superconducting phase, $YBa_2Cu_3O_{7-x}$. In the solid-state-reacted powder, $BaCO_3$ phase was observed. The superconducting transition temperatures were measured by the four-point probe technique from 77 K to room temperature for samples prepared from both powders. The resistivity versus temperature curves are shown in Fig. 2. T_c of the sinter-forged and pressureless sintered samples are 86 and 84 K, respectively. The higher resistivity of the sample from solid-state reacted powder compared to the sample from spray-roasted powder at temperatures above T_c might be related to the presence of non-superconducting $BaCO_3$ phase.

The densities of the samples which were sinter-forged for 20 h at 860, 880 and 900 °C are plotted as a function of the applied stress in Fig. 3. The relative

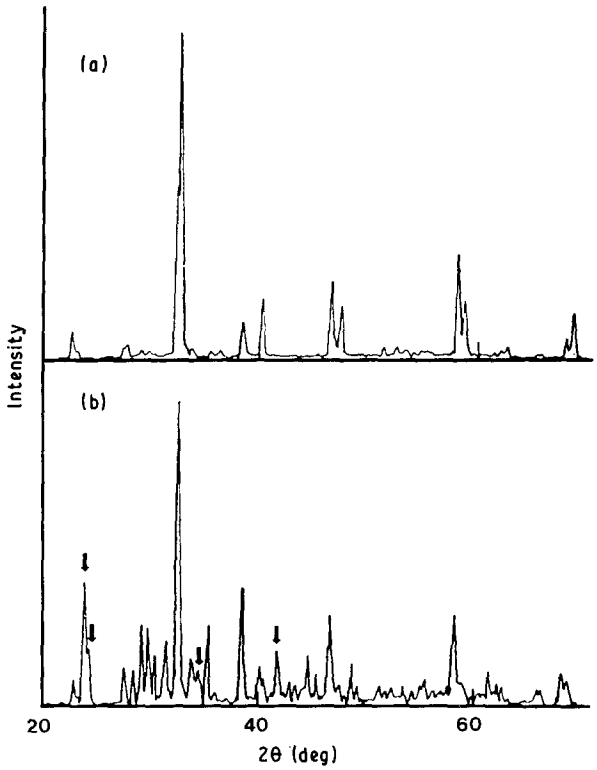

Figure 1 X-ray diffraction patterns of (a) spray-roasted powder and (b) solid-state reacted powder after calcination. The arrows indicate $BaCO_3$ peaks.

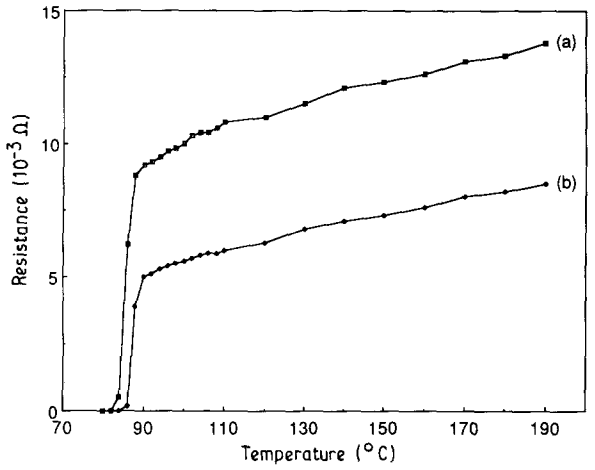

Figure 2 Resistance versus temperature curves for (a) the pressureless-sintered sample from solid-state reacted-powder and (b) the sinter-forged sample from spray-roasted powder.

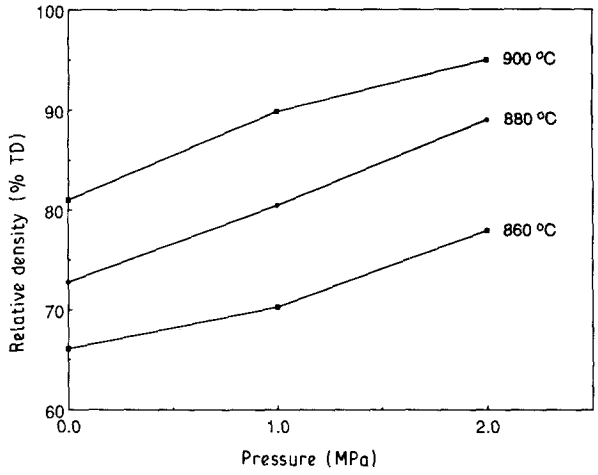

Figure 3 Variation of relative density as a function of uniaxial stress for the samples sintered for 20 h at 860, 880 and 900 °C.

density increases linearly with the applied stress. Fig. 3 also shows the improvement of the relative densities (11%–15%) due to the applied stress (2 MPa) in comparison with the pressureless sintered material. The highest density, 95% TD, was obtained by sinter-forging at 900 °C for 20 h under 2 MPa. The J_c of the sinter-forged samples was determined from typical current–voltage characteristics at 77 K using zero magnetic field. It was measured using a four-point technique. The values are summarized in Table I. The J_c values of the samples sintered at 900 °C for 20 h under 2 MPa and O MPa were 420 A cm^{-2} (the highest value) and 190 A cm^{-2}, respectively. Effects of the sinter-forging time (above 20 h) on the J_c can be ignored because of the small difference found for J_c using material which had been sinter-forged at 880 °C under 2 MPa for between 20 and 40 h. The improvement of J_c of the sinter-forged samples can be attributed to the alignment of the elongated $YBa_2Cu_3O_{7-x}$ grains.

Optical micrographs of the sinter-forged sample from the spray-roasted powder before annealing show the plate-like $YBa_2Cu_3O_{7-x}$ grains on the polished surface perpendicular to the stress axis in Fig. 4a and a textured microstructure with the alignment of the elongated grains on the surface parallel to the stress axis in Fig. 4b. The SAD pattern (Fig. 5b and c) obtained from an elongated $YBa_2Cu_3O_{7-x}$ grain in Fig. 5a reveals a parallel relationship between the *c*-axis of the grain and the stress axis. Elongation of

TABLE I Critical current densities of the sinter-forged $YBa_2Cu_3O_{7-x}$ superconductors at 77 K in zero magnetic field

Sinter-forging condition				
Stress (MPa)	Temperature (°C)	Time (h)	J_c (A cm^{-2})	Relative density (% TD)
0	900	20	190	81
2	860	20	360	78
2	880	20	365	89
2	880	40	370	–
2	900	20	420	95

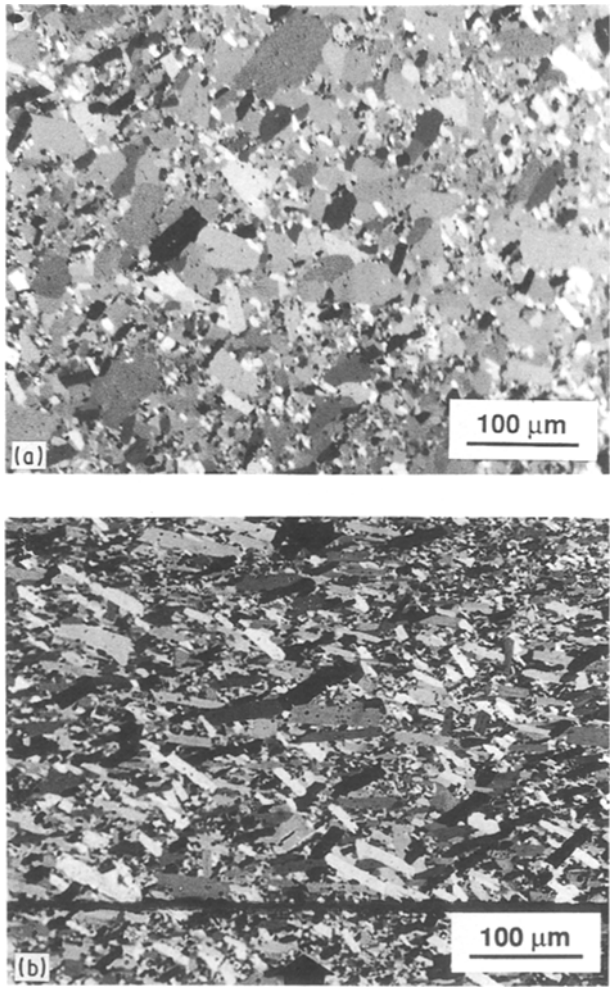

Figure 4 Optical micrographs showing (a) the plate-like $YBa_2Cu_3O_{7-x}$ grains on the polished cross-section cut perpendicular to the stress axis and (b) the alignment of the elongated grains on the cross-section cut parallel to the stress axis for the sample sinter-forged at 880 °C for 20 h under 2 MPa. The arrows in (b) show the direction of the applied stress.

$YBa_2Cu_3O_{7-x}$ grain in a direction perpendicular to the *c*-axis can be explained by a preferential movement of the (1 1 0) planes (the tetragonal phase is stable during sintering). The effect of the atomic arrangement within the tetragonal unit cell of the $YBa_2Cu_3O_{7-x}$ can be considered in a manner similar to that used to explain anisotropic growth of hexagonal ZnO grains [25]. In $YBa_2Cu_3O_{7-x}$, the (0 0 1) plane has four types of ion occupancy which repeat periodically, i.e. the Cu–O plane, the Ba–O plane, the Cu–O_2 plane, and the Y plane. Two (1 0 0) planes occur which are referred to as the $Cu_{1.5}$–$O_{2.5}$ plane and Y–Ba_2–O_2 plane. In contrast, the {1 1 0} plane has one type of plane with the atomic proportion of Y–Ba_2–$Cu_{1.5}$–O. It may thus be more favourable for {1 1 0} surface to move than surfaces parallel to other planes. During sinter-forging, the plungers are pressed together at the required temperature, allowing free movement of the specimen in the lateral direction, with slow deformation rates. Thus, the elongated $YBa_2Cu_3O_{7-x}$ grains are aligned perpendicular to the applied stress axis. Twins were also observed in the elongated grains as illustrated in Fig. 6a. Fig. 6b and c show the corresponding SAD pattern recorded for the twins with a

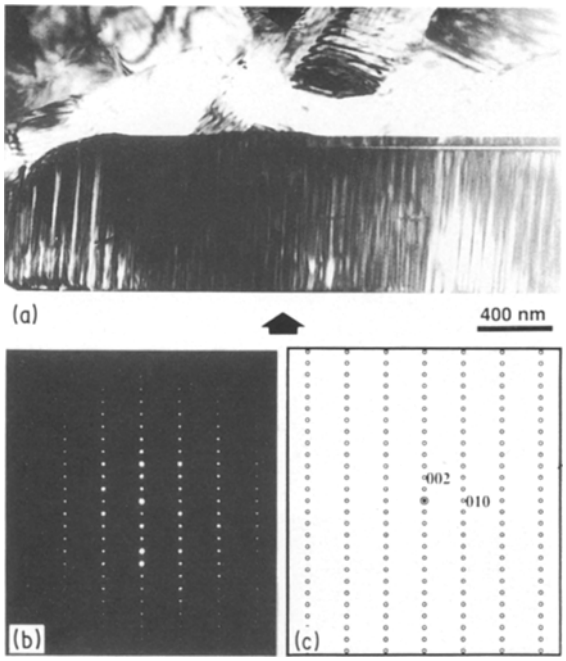

Figure 5 (a) Bright-field image showing part of an elongated $YBa_2Cu_3O_{7-x}$ grain aligned perpendicular to the stress axis in the sample sinter-forged at 880 °C for 20 h under 2 MPa, (b) SAD pattern from the elongated grain with [1 0 0] zone axis, and (c) schematic illustration of the SAD pattern. The arrows in (a) show the direction of the applied stress.

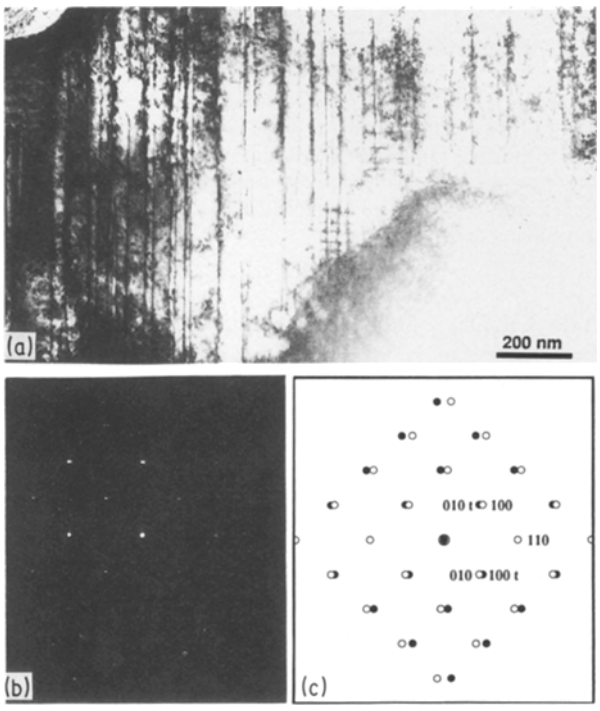

Figure 6 (a) Bright-field image showing twins in the $YBa_2Cu_3O_{7-x}$ grain of the sample of Fig. 5, (b) SAD pattern from the twins, and (c) schematic illustration of the SAD pattern demonstrating the (1 1 0) twin plane. (Note: (○) and (●) correspond to the diffracted beams from the matrix and twin of the $YBa_2Cu_3O_{7-x}$ grain with [0 0 1] zone axis.)

common [0 0 1] zone axis. The pattern reveals the same orientation relationship as the previous reports [26–28] that twin boundaries lie on the common (1 1 0) planes. In addition, Fig. 6a shows intersecting

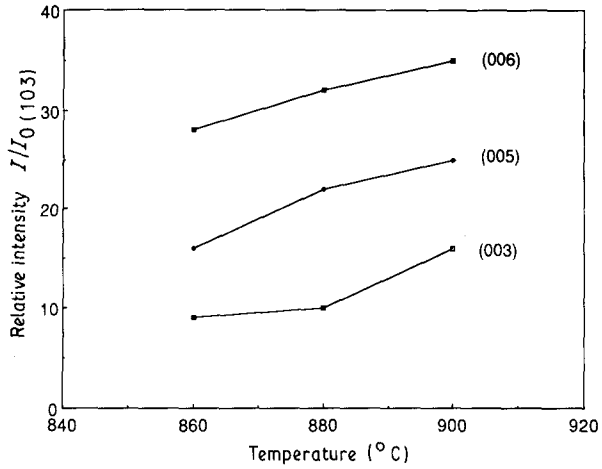

Figure 7 Variation of relative intensity $(I_{(0\,0\,x)}/I_{(1\,0\,3)}$ as a function of sintering temperature for the samples sinter-forged under 2 MPa for 20 h.

twins, i.e. twin patterns in which twin boundaries also form on the second set of {1 1 0} planes, as has been reported elsewhere [29–32].

X-ray diffraction measurement along the cross-section perpendicular to the sinter-forging axis provides a quantitative evidence of the texturing in the sinter-forged samples. Fig. 7 shows a variation in the ratio of the normalized diffracted intensity from the *c*-plane, as a function of the sinter-forging temperature. The increases of these relative intensities (Fig. 7) and the critical current densities (Table I) with the sinter-forging temperature demonstrate that the critical current density is improved by the texturing of the elongated $YBa_2Cu_3O_{7-x}$ grains.

4. Conclusions

$BaCO_3$-free and chemically homogeneous $YBa_2Cu_3O_{7-x}$ superconducting powder was obtained by the spray-roasting process from the non-carbonate precursors. The sample which was sinter-forged at 900 °C for 20 h under 2 MPa had the highest values of both the sintered density (95% TD), and J_c, 420 A cm^{-2}. The J_c values of the samples sintered at 900 °C for 20 h under 2 MPa and O MPa were 420 A cm^{-2} (the highest value) and 190 A cm^{-2}, respectively. SAD pattern obtained from elongated $YBa_2Cu_3O_{7-x}$ grains confirm that the *c*-axis of the grains and the stress axis tend to align. The elongation of $YBa_2Cu_3O_{7-x}$ grains in the direction perpendicular to the *c*-axis indicates a preferential growth of these planes which may be related to the atomic arrangement on the {0 0 1}, {1 0 0}, and {1 1 0} planes of the tetragonal unit cell. X-ray diffraction measurement along the cross-section perpendicular to the sinter-forging axis has provided quantitative evidence of the texturing in the sinter-forged samples.

Acknowledgements

The authors thank Mr Ray Coles for maintaining the Electron Microscope Facility at Cornell, Ms Margaret Fabrizio for photographic work and

Dr Stuart McKernan for valuable discussions. The electron microscopes are supported, in part, by NSF through the Materials Science Center at Cornell. This research has been supported, in part, by the Korean Science and Engineering Foundation and, in part, by the US Department of Energy (DE-FGO2-84ER45092 and DE-FGO2-89ER45381; Dr J. Routbort and Dr R. J. Gottschall).

References

1. T. R. DINGER, T. K. WORTHINGTON, W. J. GALLAGHER and R. L. STANDSTROM, *Phys. Rev. Lett.* **58** (1987) 2687.
2. G. W. CRABTREE, J. Z. LIU, A. UMEZAWA, W. K. KWOK, C. H. SOWERS, S. K. MALIK, B. W. VEAL, D. J. LAM, M. B. BRODSKY and J. W. DOWNEY, *ibid.* **B36** (1987) 4021.
3. P. CHAUDHARI, J. MANNHART, D. DIMOS, C. C. TSUEI, J. CHI, M. M. OPRYSKO and M. SCHEUERMANN, *ibid.* **60** (1988) 1653.
4. N. M. HWANG, Y. K. PARK, H. K. LEE, J. H. HAN, G. W. BANG, K. W. LEE, H. G. MOON and J. C. PARK, *J. Amer. Ceram. Soc.* **71** (1988) C210.
5. T. MATSUSHITA, B. NI, Y. SUDO, M. IWAKUMA, K. FUNAKI, M. TAKEO and K. YAMAHUJI, *Jpn J. Appl. Phys.* **27** (1988) 929.
6. Q. ROBINSON, P. GEORGOPOULOS, D. L. JOHNSON, H. O. HARCY, C. R. KANNEWURF, S. J. HWU, T. J. MARKS, K. R. POEPPELMEIER, S. N. SONG and J. B. KETTERSON, *Adv. Ceram. Mater.* **2** (1988) 380.
7. M. N. RAHAMAN, L. C. DE JONGHE and M. CHU, *ibid.* **3** (1988) 393.
8. M. H. HODGE, W. R. BITLER and R. C. BRADT, *J. Amer. Ceram. Soc.* **56** (1973) 497.
9. S. K. DEY and J. S. REED, *Amer. Ceram. Soc. Bull.* **64** (1985) 571.
10. K. R. VENKATACHARI and R. RAJ, *J. Amer. Ceram. Soc.* **69** (1986) 499.
11. M. N. RAHAMAN, L. C. DE JONGHE and C. H. HSUEH, *ibid.* **69** (1986) 58.
12. M. N. RAHAMAN, L. C. DE JONGHE and R. J. BROOK, *ibid.* **69** (1986) 53.
13. A. G. EVANS, *ibid.* **65** (1986) 497.
14. R. RAJ, *ibid.* **65** (1982) C-46.
15. R. R. NEURGAONKAR, G. SHOOP, J. R. OLIVER and I. SANTHA, A. S. BHALLA and L. E. CROSS, *Mater. Res. Bull.* **23** (1988) 143.
16. R. E. LOEHMAN, W. F. HAMMETTER, E. L. VENTURINI, R. H. MOORE and F. P. GERSTLE Jr, *J. Amer. Ceram. Soc.* **72** (1989) 669.
17. K. SADANANDA, A. K. SINGH, M. A. IMAN, M. OSOFSKY, V. LE TOURNEAU and L. E. RICHARDS, *Adv. Ceram. Mater.* **3** (1988) 524.
18. I.-W. CHEN, X. WU, S. J. KEATING, C. Y. KEATING, P. A. JOHNSON and T.-Y. TIEN, *J. Amer. Ceram. Soc.* **70** (1987) C-388.
19. K. A. JOHNSON, K. P. STAUDHAMMER, W. J. MEDINA, C. B. PIERCE and N. E. ELLIOTT, *Scripta Metall.* **22** (1988) 1689.
20. M. K. MALIK, V. D. NAIR, A. R. BISWAS, R. V. RAGHAVAN, P. CHADDAH, P. K. MISHRA, G. R. KUMAR and B. A. DASANNACHARYA, *Appl. Phys. Lett.* **52** (1988) 1525.
21. K. SALAMA, V. SELVAMANICKAM, L. GAO and K. SUN, *ibid.* **54** (1989) 2352.
22. N. M. ALFORD, J. D. BIRCHALL, W. J. CLEGG and K. KENDALL, *J. Appl. Phys.* **65** (1989) 2856.
23. S. JIN, T. H. TIEFEL, R. C. SHERWOOD, M. E. DAVIS, R. B. VAN DOVER, G. W. KAMMLOTT, R. A. FASTNACHT and H. D. KEITH, *Appl. Phys. Lett.* **52** (1988) 2074.
24. S. JIN, T. H. TIEFEL, R. C. SHERWOOD, R. B. VAN DOVER, M. E. DAVIS, G. W. KAMMLOTT and R. A. FASTNACHT, *Phys. Rev.* **B37** (1988) 7850.
25. G. Y. SUNG and C. H. KIM, *Adv. Ceram. Mater.* **3** (1988) 604.
26. R. BEYERS, G. LIM, E. M. ENGLER, R. J. SAVOY, T. M. SHAW, T. R. DINGER, W. J. GALLAGHER and R. L. SANDSTROM, *Appl. Phys. Lett.* **50** (1987) 1918.
27. Y. SYONO, M. KIKUCHI, K. OHISHI, K. HIRAGA, H. ARAI, Y. MATSUI, N. KOBAYASHI, T. SASAOKA and Y. MUTO, *Jpn J. Appl. Phys.* **26** (1987) L498.
28. G. VAN TENDELOO, H. W. ZANDBERGEN and S. AMELINCKX, *Solid State Commun.* **63** (1987) 389.
29. M. HERVIEU, B. DOMENGES, C. MICHEL, G. HEGER, J. PROVOST and B. RAVEAU, *Phys. Rev.* **B36** (1987) 3920.
30. S. IIJIMA, T. ICHHASHI, Y. KUBO and J. TABUCHI, *Jpn J. Appl. Phys. Pt* 2 **26** (1987) L1478.
31. M. SARIKAYA, R. KIKUCHI and I. A. AKSAY, *Physica C* **152** (1988) 161.
32. T. M. SHAW, S. L. SHINDE, D. DIMOS, R. F. COOK, P. R. DUNCOMBE and C. KROLL, *J. Mater. Res.* **4** (1989) 248.

Received 11 October
and accepted 21 November 1989